

Table DR1. Physical properties of Australasian microtektites from Core SO95-17957-2, South China Sea and their mineral inclusions as detected by synchrotron X-ray diffraction and microanalytical FEG-SEM.

<i>sample</i>	<i>shape</i>	<i>color</i>	<i>transparency</i>	<i>vesicles</i>	<i>size</i>	<i>mineral inclusions</i> [†]	<i>main diffraction features</i>
1	sphere	pale yellow	transparent		515	qtz	few streaked spots along a qtz ideal ring
2	prolate ellipsoid	pale yellow	transparent	abundant	625 x 475	-	no diffraction features
4	truncate dumbbell	pale brown	transparent	abundant	740 x 400	qtz, ox	few streaked spots along a qtz ideal ring
5	sphere	brown	transparent	abundant	550	qtz, ox	fairly continuous qtz rings with streaked spots
8	brocken sphere	pale brown	translucent	abundant	459	qtz, ox, zr	fairly continuous qtz rings with few streaked spots
10	sphere	brown	translucent	abundant	370	qtz, ox	fairly continuous qtz rings with streaked spots
11	sphere	pale brown	translucent	abundant	343	qtz	few streaked spots along an ideal qtz ring
12	prolate ellipsoid	brown	translucent	abundant	591 x 495	qtz, ox	few streaked spots along an ideal qtz ring
13	truncated dumbbell	pale brown	translucent		620 x 350	qtz, ox	fairly continuous qtz rings without spots
14	angular	pale brown	transparent	abundant	583 x 482	qtz, ox	fairly continuous qtz rings with few streaked spots
16	truncated teardrop	brown	translucent	abundant	370 x 250	qtz, ox	fairly continuous qtz rings without spots
17	angular	pale yellow	translucent		596 x 461	-	no diffraction features
19	brocken sphere	brown	translucent		635	qtz, ox	few streaked spots along an ideal qtz ring
21	dumbbell	pale yellow	transparent	abundant	719 x 401	-	no diffraction features
24	sphere	brown	transparent		410	qtz, ox	few streaked spots along an ideal qtz ring

[†] Only quartz was identified by X-ray diffraction; note, however, that microtektite #12 shows also a diffraction peak at $d = 4.05 \text{ \AA}$, close to the strongest diffraction peak of cristobalite (PDF 39-1425), with $d = 4.04 \text{ \AA}$. Abbreviations: qtz = quartz; ox = Fe-oxide; zr = unidentified zr-phase.

Table DR2. Bulk composition of normal Australasian microtektites from Core SO95-17957-2 (South China Sea), obtained by averaging three 20 x 20 μm raster EPMA of sectioned microtektites. Compositions are listed in order of increasing silica content. Bulk composition of representative lechatelierite and quartz inclusions, and Al-rich glass domains observed in some microtektites are also reported. Detection limits (wt%) for the analyzed oxides are as follows: $\text{Na}_2\text{O} = 0.05$, $\text{MgO} = 0.02$, $\text{Al}_2\text{O}_3 = 0.09$, $\text{SiO}_2 = 0.06$, $\text{K}_2\text{O} = 0.06$, $\text{CaO} = 0.06$, $\text{TiO}_2 = 0.09$, $\text{Cr}_2\text{O}_3 = 0.19$, $\text{MnO} = 0.12$, $\text{FeO} = 0.16$; $\text{NiO} = 0.19$; $\text{Cl} = 0.7$). Cr_2O_3 and NiO were always below detection limits.

<i>sample</i>	<i>mount</i>	<i>SiO₂</i>	<i>TiO₂</i>	<i>Al₂O₃</i>	<i>FeO</i> [^]	<i>MnO</i>	<i>MgO</i>	<i>CaO</i>	<i>Na₂O</i>	<i>K₂O</i>	<i>total</i>
microtektites											
1	24	63.1	0.98	20.4	6.09	<i>bdl</i>	2.95	2.59	0.98	2.68	100.0
24	28	63.2	0.92	19.5	6.45	<i>bdl</i>	3.17	2.44	1.07	2.85	99.7
16	23	63.5	0.95	19.3	6.26	<i>bdl</i>	2.84	2.61	1.20	3.33	100.0
2	27	64.0	0.96	19.6	6.32	<i>bdl</i>	2.92	2.43	1.09	2.89	100.2
5	20	64.0	0.94	19.7	6.21	<i>bdl</i>	2.93	2.57	1.10	2.87	100.4
11	32	64.2	0.94	18.9	6.01	<i>bdl</i>	2.84	3.11	1.11	3.11	100.3
8	21	64.4	0.94	19.7	5.75	<i>bdl</i>	2.83	2.68	1.02	2.78	100.2
14	26	65.1	0.94	16.6	6.50	<i>bdl</i>	3.65	3.47	1.40	2.34	100.1
21	29	67.3	0.86	15.9	5.63	<i>bdl</i>	2.98	2.85	1.45	2.76	99.8
4	19	67.3	0.88	16.9	5.44	<i>bdl</i>	2.80	2.83	1.21	2.68	100.2
17	30	68.6	0.85	15.2	5.36	<i>bdl</i>	2.74	2.94	1.42	2.81	100.0
10	25	69.4	0.81	14.8	5.01	<i>bdl</i>	2.68	2.72	1.56	2.82	99.9
13	22	71.6	0.76	13.0	5.40	<i>bdl</i>	3.20	2.15	1.32	2.41	100.0
12	31	71.9	0.75	13.1	5.25	<i>bdl</i>	2.91	2.62	1.44	2.46	100.5
19	33	72.9	0.72	12.5	4.66	<i>bdl</i>	2.94	2.08	1.73	2.81	100.4
lechatelierite inclusions											
13	22	97.8	0.10	1.28	0.77	<i>bdl</i>	0.26	0.22	0.10	0.43	101.0
14	26	100.2	<i>bdl</i>	<i>bdl</i>	<i>bdl</i>	<i>bdl</i>	<i>bdl</i>	<i>bdl</i>	<i>bdl</i>	<i>bdl</i>	100.2
quartz inclusions											
14	26	100.6	<i>bdl</i>	<i>bdl</i>	<i>bdl</i>	<i>bdl</i>	<i>bdl</i>	<i>bdl</i>	<i>bdl</i>	<i>bdl</i>	100.6
14	26	100.2	<i>bdl</i>	<i>bdl</i>	<i>bdl</i>	<i>bdl</i>	<i>bdl</i>	<i>bdl</i>	<i>bdl</i>	<i>bdl</i>	100.2
schlieren											
13	22	54.4	0.59	18.1	12.0	0.16	6.69	6.24	0.83	1.06	100.3

[^]All Fe given as FeO.

Fig. DR1. Harker diagrams for Australasian microtektites from Core SO95-17957-2 (South China Sea) compared to Australasian microtektites from literature distinguished by chemical groups established by Glass et al. (2004).

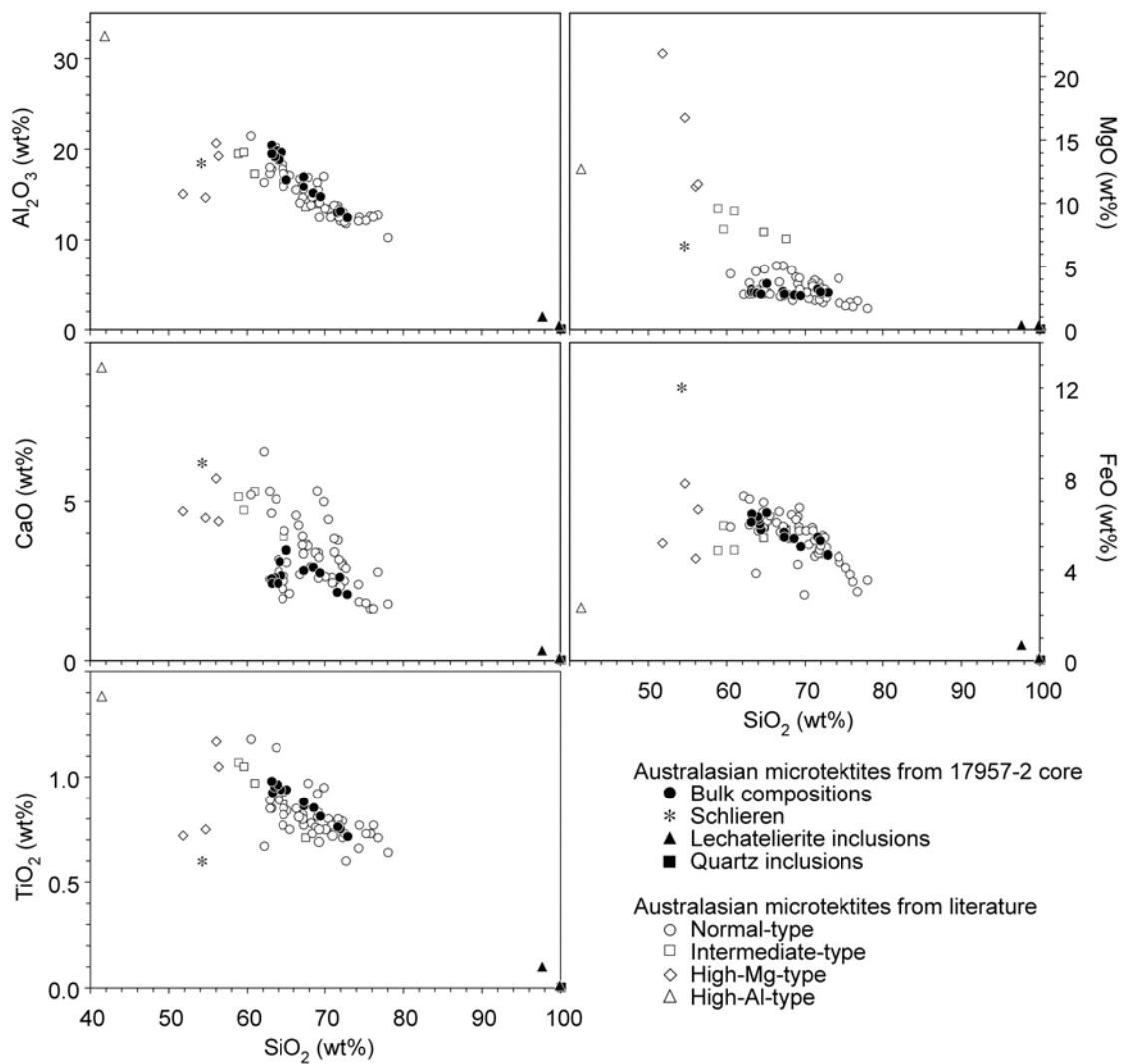


Fig. DR2. A further example of synchrotron X-ray diffraction pattern of an Australasian microtektite from Core SO95-17957-2 (microtektite #12) showing streaked diffraction maxima along fairly continuous diffraction rings resulting from shocked quartz crystals with moderate to strong mosaicism (white labels). The diffraction pattern also shows faint diffraction maxima at $d = 4.05 \text{ \AA}$, close to the strongest diffraction peak of cristobalite (PDF 39-1425), with $d = 4.04 \text{ \AA}$ (black label).

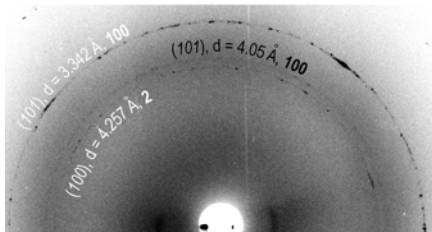


Fig. DR3. EDS spectra of the yet to be identified Zr-phase featured in Fig. 3E found in Australasian microtektite #8 from Core SO95-17957-2 (South China Sea).

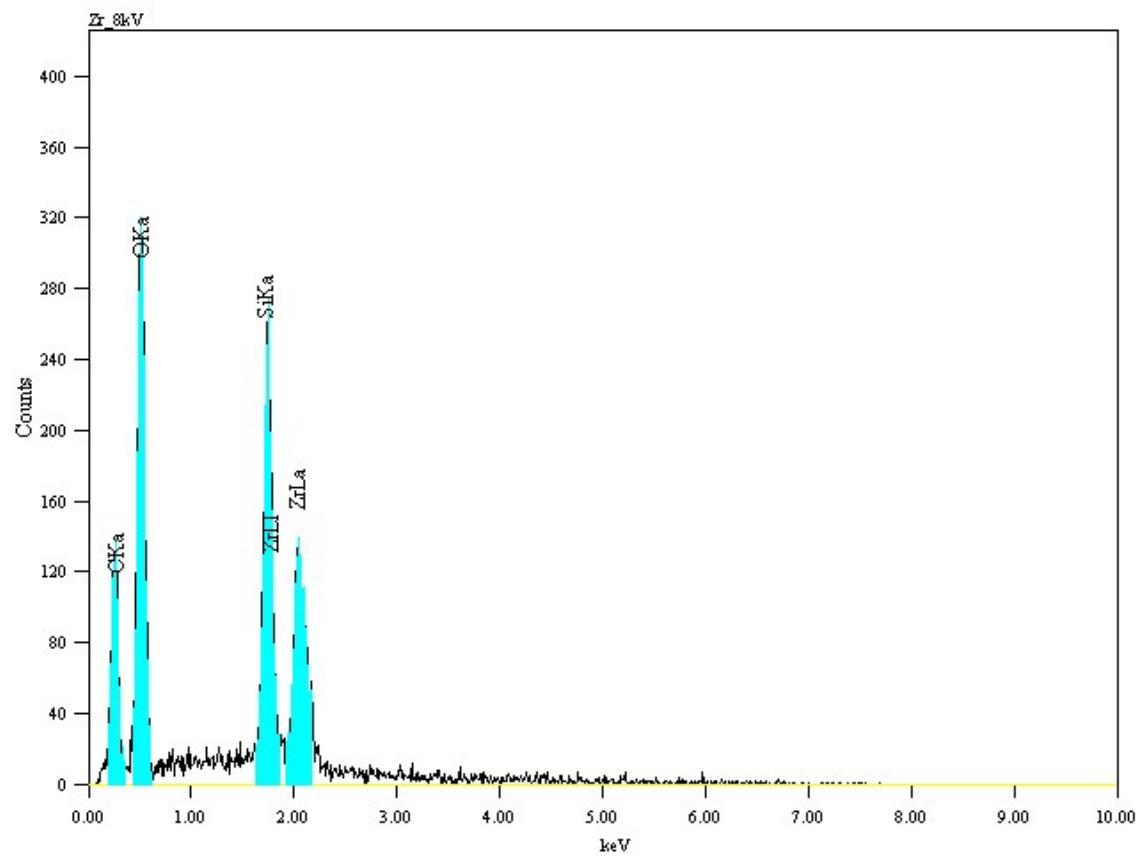


Fig. DR4. Micrograph of a sectioned Australasian microtektite from Hole ODP 769A core (Sulu Sea) showing abundant quartz inclusions. Quartz crystals are often associated with lechatelierite (silica glass), opaque crystallites and vesicles. Abbreviations: qtz = quartz; gl = glass; op = opaque; v = vesicles.



Fig. DR5. Raman spectrum of a α -quartz grain found in the Australasian microtektite featured in Fig. DR3. The main wavelengths of α -quartz are reported in black. Additional features include a shoulder at 447 cm^{-1} , probably due to the presence of rutile, and a weak band at 1000 cm^{-1} , attributed to silica-rich glass. The fluorescence of the spectrum is generated by the resin mount. Note the broadening and downshift of the A1 mode at 465 cm^{-1} in the Raman spectra of the α -quartz, which might be indicative of an increased spread of Si-O-Si angles caused by a progressive and important shock induced distortion of the structural configuration. Raman spectra and was acquired with a Jobin Yvon Labram microprobe, equipped with a Peltier-cooled CCD detector and a 514.5-nm argon-ion laser at the Earth Sciences department of Siena University. The measured laser power of the polarized 514.5-nm excitation line was 300–500 mW at the source and about 80% less at the sample surface. The slit width was $100\text{ }\mu\text{m}$, and the corresponding spectral resolution was 1.5 cm^{-1} . Raman spectra were collected through a $100\times$ Olympus objective (excitation spot 1–2 μm in diameter) for a short acquisition time (30 or 60 s for each spectrum). Frequency Wavenumbers of the Raman lines were daily calibrated by the position of the diamond band at $1,332\text{ cm}^{-1}$.

